BACHELOR

Interferometric particle imaging in turbulent flow

de Vrieze, P.

Award date:
2013

Interferometric particle imaging in turbulent flow

P de Vrieze

August 29, 2013

R-1828-S

Abstract

Turbulence plays a large role in the formation of droplets in atmospheric clouds. We create turbulence in a box using synthetic jets, and find the droplet sizes using interferometric particle imaging (IPI). To analyse the images obtained, a few different methods have been tried, which eventually led to the creation of a program which uses the wavelet transform to find the droplets, and Fourier analysis and a least-squares fit to find their size.
The question is how the particle size PDF depends on the turbulence conditions. To this aim we have measured the particle size PDF using three different scenarios; one with a continuous flow of droplets coming into the turbulent flow, one where the flow of droplets is cut off after a while and one without turbulence where droplets are added during the measurement. We have observed a large effect of the particle inertia on turbophoresis so that the flux of large droplets towards the walls of the box is much larger than that of small droplets.

Contents

1 Introduction

Small droplets which are illuminated by coherent light create an interference pattern resulting from rays passing over and through the droplet. These interference patterns are made visible by out-focus imaging of the droplets: each droplet corresponds to a disk in the image plane whose diameter is determined by the lens aperture. To calculate the size of the droplets in the image, two challenges are presented: finding the position of the disks, and finding the frequency of it's fringes. The first has been attempted in different ways: using a Hough Transform to find elliptic shapes, finding connected pixels and eventually a wavelet transform. Then once the disks have been found, finding the fringes frequency has been attempted by calculating the distance between it's maxima, by using a Fourier transformation of the signal and by computing a least-squares fit on the signal. Eventually, a combination of the last two was used, to find an approximation of the variables and improve them with the least-squares fit.
Once a method to calculate the particle size distribution function (PDF) had been found, several experiments have been performed. The first one was a measurement of the PDF's while droplets were continuously added to the turbulent flow. In the second experiment the influx of droplets was terminated halfway during the experiment, to take a look at the decrease of the amount of droplets. Finally, PDF's were examined inside the box without any turbulence, and just a constant influx of droplets.

2 Theory

2.1 Cloud dynamics

In atmospheric clouds, there is a large range of spatial scales present. The properties of such clouds are defined by its properties from micrometer scales to meter scales. Turbulence on these scales results in a Reynolds number in the order of 10^6 to 10^7. This report will only look in to small scales of cloud dynamics, it is these microscale properties that affect the efficiency of rain production in clouds. Those properties are determined mainly by thermodynamic and fluid-mechanical interactions between droplets and surrounding air. It is expected that fine-scale turbulence is of direct importance to the evolution of the droplet size distribution in a cloud, which has been the main area of interest of this research project. [1]
The dynamics of a cloud can be reproduced in the laboratory inside a small box in which turbulence is created and small water droplets are released. The particles can be visualized by shining a laser sheet through it, a camera can then pick up the reflections from the droplets. Inside this box however, the droplets will interact with the wall and with each other, both effects will be described here.

Wall collisions

It is assumed, that when a droplet hits the wall, it sticks on the wall and will not come back into the region where measurements take place. This means that the amount of droplets will decrease over time. The rate q at which these collisions take place depend on the surface area A, the volume V and the root mean square velocity of the particles u_{rms} as:

$$q = \frac{u_{rms} N A}{V}. \tag{1}$$

Which can be written into a differential equation for the number of particles:

$$\frac{dN}{dt} = -q = -\frac{u_{rms} N A}{V}. \tag{2}$$

The solution to this differential equation is:

$$N = \exp\left(-\frac{t}{\tau}\right) + C, \tag{3}$$

with

$$\tau = \frac{V}{u_{rms} A}. \tag{4}$$

It is hard to determine the amount of particles in the cloud, but assuming the total intensity of the reflected laser light is linearly related to the amount of particles the constant τ can now be found from an intensity measurement over time. The intensity however will also be dependant on the particle sizes, the intensity is a decent measure for the total amount of particles, but it is not perfect.

Particle collisions

Consider N spherical particles with radius r in a volume V. Suppose only one particle is moving, when it collides with another particle, the distance between centers is $2r$. Suppose we draw a cylinder with radius wr, the moving particle collides with any other particle whose center is inside this cylinder. In a short time dt the particle with speed v travels a distance $v\ dt$. During this time it collides with any molecule that is in the cylindrical volume of radius $2r$ and length $v\ dt$. In a box with N/V particles per unit volume, the mean free time τ_m will be

$$\tau_m = \frac{V}{N \pi r^2 v}. \tag{5}$$

This result assumes that only one particle is moving. In the case where all particles are moving in random directions, the chance of a collision increases by a factor $\sqrt{2}$:

$$\tau_m = \frac{V}{\sqrt{2} N \pi r^2 v}. \tag{6}$$

2.2 Interferometric particle imaging

Interferometric particle imaging (IPI) is a technique which is based on the interference between the reflection and first-order refractive scattering from spherical particles. The origins of IPI can be found in König *et al.*(1986), where a single laser beam was focused onto a stream of droplets and the resulting fringe pattern was measured [2]. In this case, we use a laser sheet to illuminate droplets on a two dimensional plane. A droplet will reflect

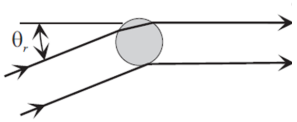

Figure 1: Reflection and refraction on a droplet

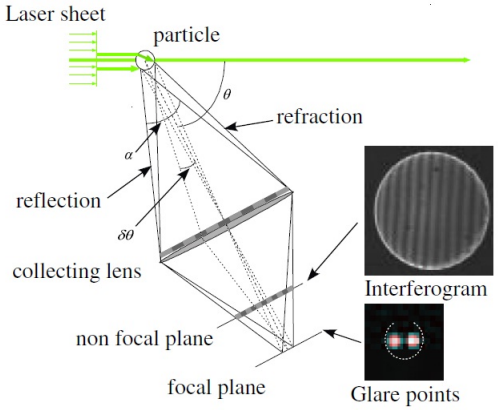

Figure 2: Basic configuration of the IPI system[4].

this light, and a first order refraction will pass through the droplet, which creates two glare points, as seen in Figure (1). When taking an out of focus image, the two glare spots will interfere with each other and create an interferogram, as shown in Figure (2). The interferogram size depends on the size of the aperture of the camera, and not on the particle size, so all the interferograms of different particles will be of equal size. The fringe spacing is proportional to the droplet diameter. A derivation of the difference in optical path lengths of the two rays can be found in Albrecht *et al.*[3]. The angular separation $\Delta\phi$ of the fringes is determined by the optical path length difference of the two scattered rays,

$$\Delta\phi = \frac{2\lambda}{A(\theta_r)d_p}, \tag{7}$$

with d_p the particle diameter and λ the wavelength of the incident light. The factor $A(\theta_r)$ reflects the geometry of the two rays passing through and over the droplet:

$$A(\theta_r) = \left(m\cos(\theta_r/2) + \frac{m\sin(\theta_r)}{\sqrt{m^2+1-2m\cos(\theta_r/2)}} \right). \tag{8}$$

With m the relative refractive index and θ_r the angle between the optical axis of the system and the incident light. Angular information of the scattered light can be obtained from the fringe spacing Δx in the out-focus image:

$$\Delta x = (d_i/d_a)v\Delta\phi \tag{9}$$

with d_i the diameter of the circular disk representing a particle in the image, d_a the diameter of the aperture and v the object distance.
In this "conventional" IPI method, the interferograms will be depicted as circles, or squares, depending on the aperture shape. At higher particle concentrations, the patterns will start overlapping, making it difficult to measure the fringe spacing from the image, as can be seen in Figure (3A). By defocusing in the horizontal direction, and focusing in the vertical direction, these circles or squares can be compressed to ellipses or long rectangles. This greatly reduces the area covered by the interference pattern, and therefore reduces the amount of overlap in the image.

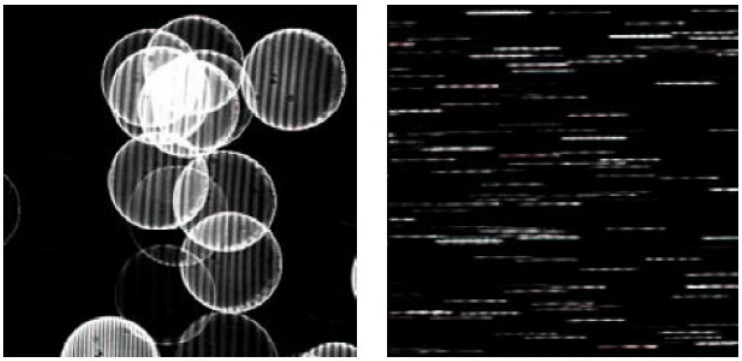

(A) (B)

Figure 3: An example of an IPI image. (A) Using the conventional technique, even a few particles will overlap. (B) By just defocusing in one direction, more particles can be identified [4].

2.3 Mie scattering

The interference patterns resulting from refraction and reflection in the droplets can be calculated using Mie scattering. This is the solution to Maxwell's equations found by Gustav Mie. A program called MiePlot can calculate and show the Mie scattering for different particle sizes, laser wavelengths and polarisation. Using a perpendicularly polarized green laser beam with a wavelength of $\lambda = 532$ nm, and a radius of $r = 5\mu$m results in Figure (4). It is easier to compare these results in a Cartesian coordinate system. The results for different radii are shown in Figure (5). If both the reflective and refractive ray from the droplet has the same intensity,

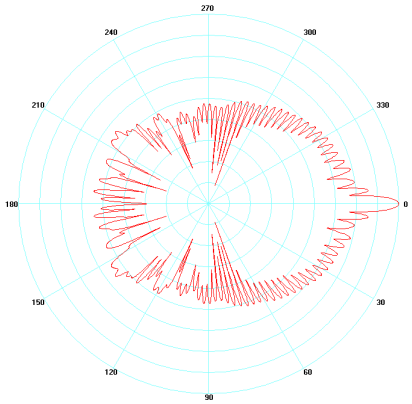

Figure 4: Example of a polar plot of Mie scattering on a logarithmic scale. The laser hits the particle at an angle of 180°.

it will create a nice fringe pattern with equally large fringes. This depends on both the particle size and the scattering angle, if for instance the intensity of a particle with $r = 5$ μm is measured from an angle of about 110°, the interference pattern will not have the same intensity along the interferogram, there is a factor 10 difference between some of the peaks in the measured region, as seen in Figure(6). This will make it hard to find the fringes from the image by fitting a cosine function through the intensity along the interferogram, or by finding the maxima in the image. Another way to find the fringe spacing is by using a Fourier Transform on the intensity profile along a horizontal line through the interferogram.

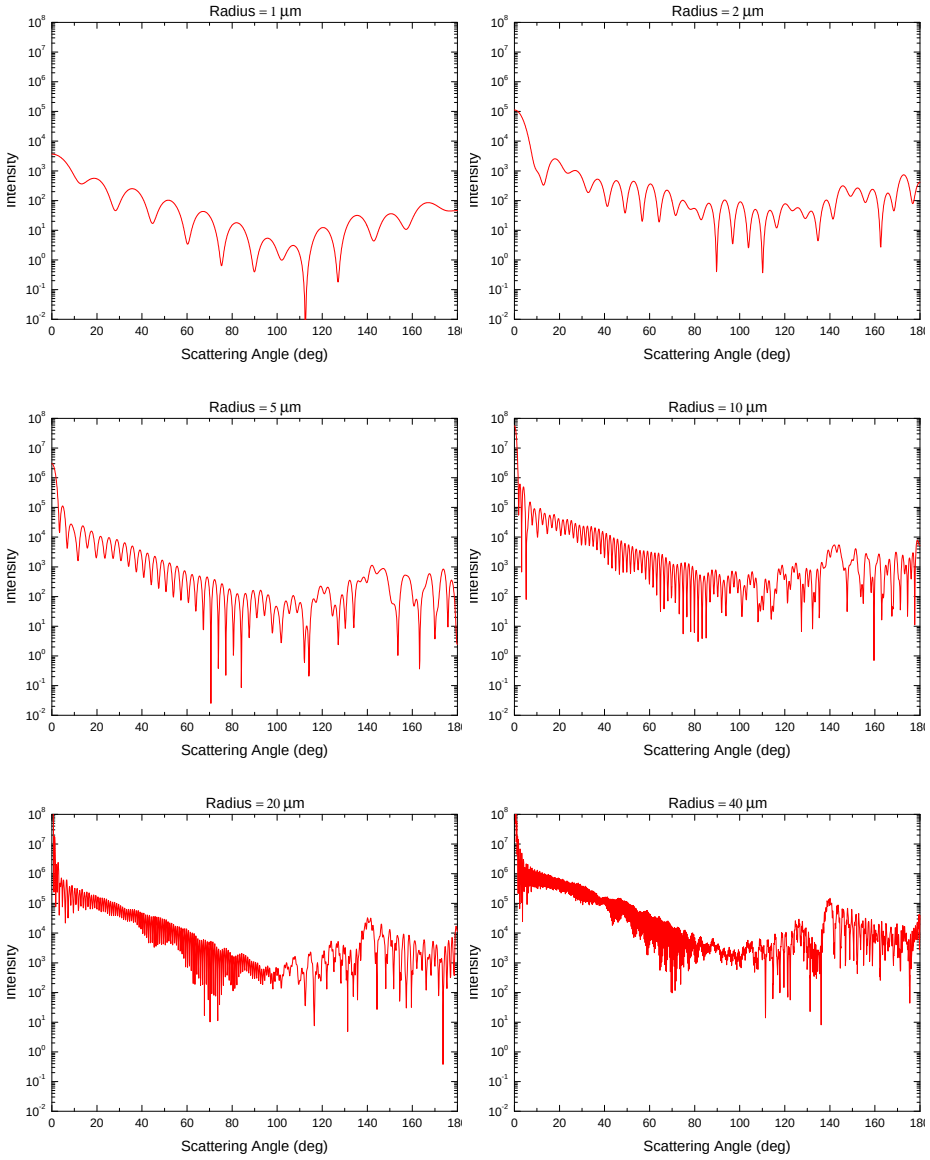

Figure 5: Mie plots for different particle sizes.

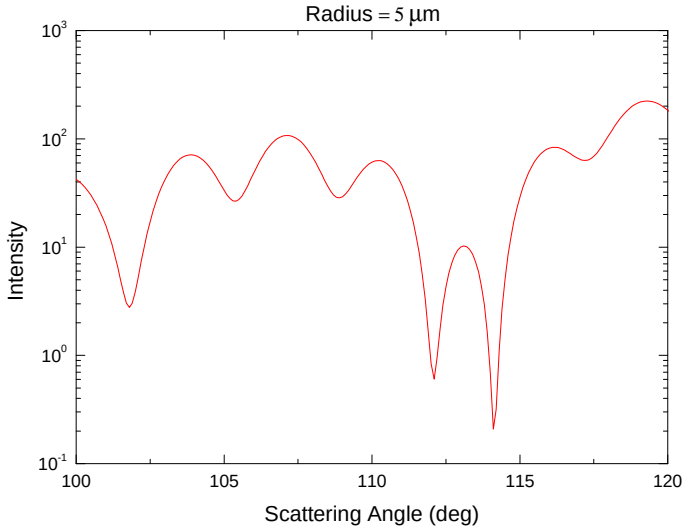

Figure 6: Mie plot of a particle with $r = 5$ μm, zoomed in between 100° and 120°.

2.4 Spinning disk sprayers

A spray of almost uniform drop size can be formed when liquid is fed to the centre of a rotating disk and centrifuged off the edge [9]. With this method, homogeneous clouds in the drop-size range from 3 mm to 15 μm can be created. The size of the spray drops is inversely proportional to the angular velocity of the disc. To produce relatively coarse sprays, a motor-driven disc can suffice. But finer spray sizes require rotor speeds up to several thousands of revolutions per second, which can be reached by using air driven "tops". At very high rotational speeds, not only a homogeneous spray is formed, but the cloud also contains smaller satellite droplets. The primary diameter d of the droplets can be calculated with [10]:

$$d = \frac{Qu}{\sqrt{R\rho/\sigma\omega}}, \tag{10}$$

where R is the disk radius, ρ the fluid density and σ is it's surface tension. ω is the angular velocity of the spinning disk and Qu is a number that depends weakly on the supply rate Q of the fluid:

$$Qu = \frac{1}{8}(\log Qe + 2.85)^2 + 2.15 \tag{11}$$

where Qe is the dimensionless flow rate formed from Q and a reference value for a thin film driven by a centrifugal force:

$$Qe = \frac{Q}{2\pi R^2\sqrt{\nu\omega}} \tag{12}$$

with ν the kinematic viscosity of the fluid.
We are interested in droplet sizes between 10 μm and 60 μm. Given that our spinning disk has a maximum angular velocity of 3600 s^{-1}, we must reduce the surface tension of water in order to achieve these diameters. By adding Triton-X100 at a 1% by volume achieves a surface tension of $\sigma = 3 \cdot 10^{-2}$ N/m.

3 Experimental setup

As mentioned in section 2.1, the dynamics of a cloud can be reproduced in a small box. In this case a cubic box with sides of 40cm is used. 8 synthetic jet speakers on the corners of this box generate the required turbulence inside by producing noise (Figure 7). A high frequency pulsed laser beam with wavelength $\lambda = 532$ nm, diverged by a negative lens with focal length $f = 55$ mm, is led through the box, lighting up the particles on a plane. A camera perpendicular to the lasersheet can now take images of the particles in that plane. When the camera is focused on the plane, the images can be used to determine the velocities of the particles, by Particle Image Velocimetry. When the laser sheet is outside of the plane of focus of the camera, the interference patterns mentioned in section 2.2 can be used to determine the size of the particles.

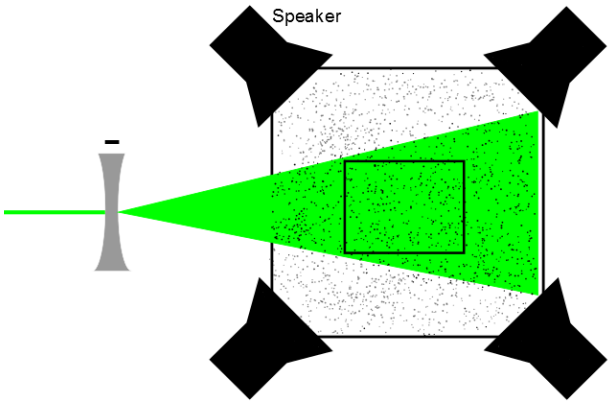

Figure 7: 2D sideway view of the setup

In our experiments turbulence was created by the speakers with 20 Hz noise. This creates a turbulence whose properties are listed in table 1. u_{rms} is the root mean square velocity of the particles, v_k the Kolmogorov velocity and Re_λ the turbulent Reynolds number.

Table 1: Properties of the turbulence inside the box

u_{rms}	1,73 m/s
v_k	$3,134 \cdot 10^{-2}$ m/s
Re_λ	369

4 Data analysis

Once the images with the fringe patterns for each droplet have been acquired, the size of the droplets needs to be computed. This requires a method that can quickly and efficiently find all droplets, take the intensity along it's fringe pattern, and calculate the spatial frequency of the fringes. In this project, different methods have been examined, which will be discussed below.

4.1 Finding the particles

Randomized Hough transform

When a circular aperture is used, the fringe patterns will be elliptical. To find ellipses in an image, a technique called Randomized Hough transform can be used. The regular Hough transform (HT) is a standard technique for detecting curves in an image [7]. The HT consists of three steps: 1. a pixel in the image is transformed into a parametrised curve, 2. valid curves parameters are binned into an accumulator where the number of curves in a bin equals its score, and 3. a curve with a maximum score is selected from the accumulator to represent a curve in the image. This method requires a large accumulator and much processing time. To reduce these problems Xu *et al.*proposed a Randomized Hough transform (RHT). When applied to find ellipses, this technique randomly selects three nonzero pixels in an image. By filtering the image in a way where only the edges of the ellipse are nonzero, the RHT will select three pixels on the edge of one of the ellipses. It then defines lines tangent to the edge at the location of each of the three pixels. If these three lines intersect, the bisectors of the two intersection points are taken. These lines will intersect in the center of the ellipse as can be seen in Figure 8:

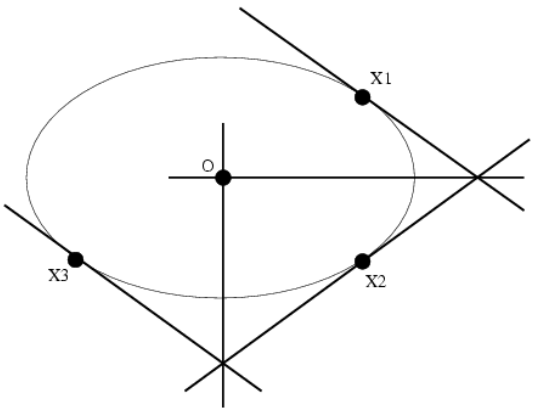

Figure 8: Determining an ellipse center, which is located at the intersection of the bisections of the three tangents to the ellipse.

Since this technique uses random points in the image, there is only a small chance this all works out. All three random points need to be on the same ellipse and they need to be far enough away from each other so the bisectors can be calculated accurately. To improve the chance of success, the algorithm simply repeats this and keep the ellipses that best match the ellipse in the image. This method works fine for an image with a few ellipses, but logically, the chances of success decrease rapidly with an increasing number of ellipses in the image. Besides the fact that there are usually between 5 and 20 ellipses in an image, the shape of the ellipses also make it hard for this technique to work well. The ellipses are very thin and long stretched, which often results in two almost parallel lines. The bisector of these lines is then very inaccurate which will not result in the correct centerpoint.

Connected pixels

Another method to find the particles is by looking at connected pixels. This method will also work on other shapes then just ellipses. So if a squareshaped aperture is used, the resulting rectangular fringe patterns (Figure 9) can also be found.

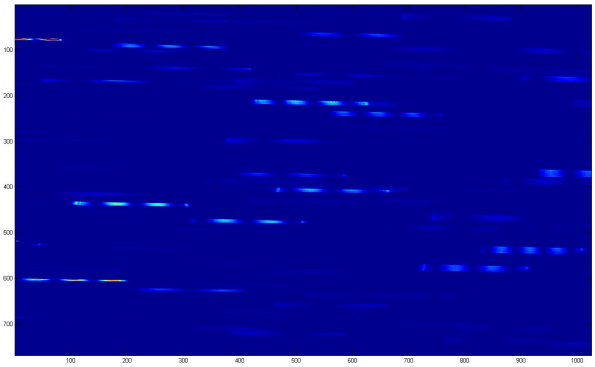

Figure 9: Original image taken with square aperture, the vertical focusing results in long-stretched rectangular fringe patterns.

The original image first needs to be filtered so that every point on an ellipse has a nonzero value, and all points outside of the ellipses equal zero. The exact details of these filters can be found in Appendix 1.1, and they result in Figure 10:

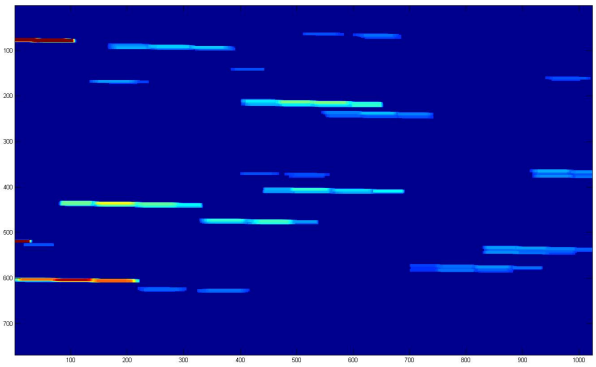

Figure 10: The image after applying several filters

After filtering, each group of connected pixels will be labeled with a different index, which makes it easy to work with each group seperately. The result of this labeling is shown in Figure 11:

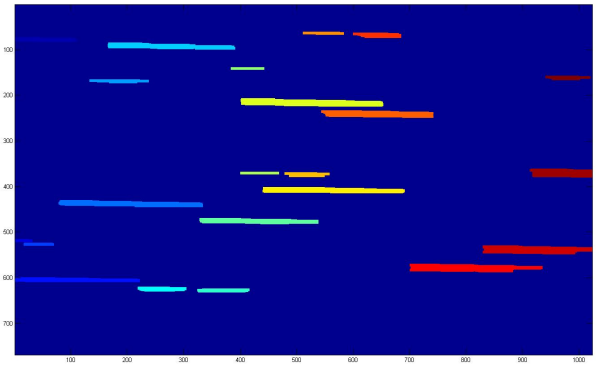

Figure 11: The image after labeling, each group of connected pixels is given another color

As can be seen from the image, there are some smaller groups of connected pixels, which do not match with entire particles. Because the fringe pattern was too weak, the part in between two fringes has been filtered out. To prevent these parts from being used in the analysis only pixel groups of at least a certain size will be used. The center of the remaining rectangles can be found by calculating the middle of the minimum and maximum coordinates of the group of pixels. This method works fairly well to find the particles fringe patterns from the image. An example of the result is given in Figure 12.

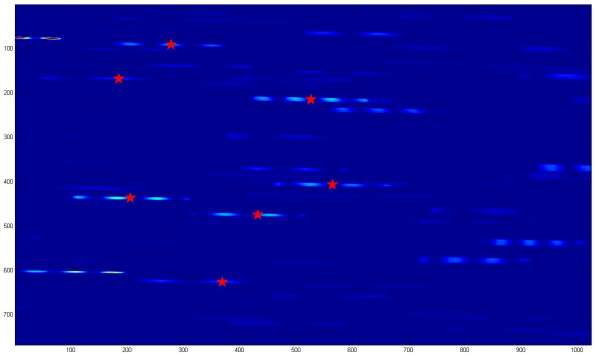

Figure 12: Result of the connected pixels method, each red star marks the center of an ellipse.

Wavelet transform

Another method to find objects in an image is the wavelet transform. This method works best with circles, so the image needs to be out of focus in both directions, which results in Figure 13

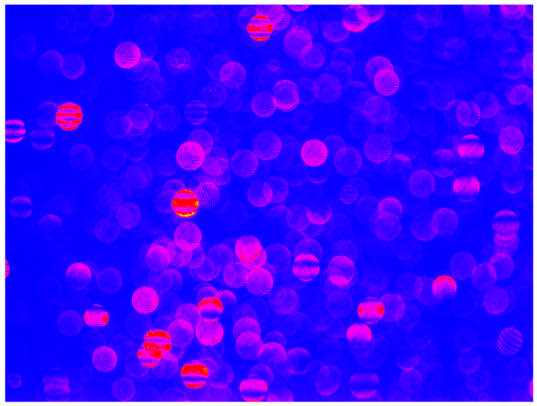

Figure 13: Original image on which the wavelet transform method is applied

All particles in the image will have the same diameter d_i. so we can convolve the image with a kernel $\kappa(x, y)$=1 if $x^2 + y^2 < (d_i/2)^2$, and 0 otherwise. Doing this results in an image with maxima at the centres of the disks. Next we seek for the local maxima in the convolved image. A center pixel (x_0, y_0) is a local maximum if its

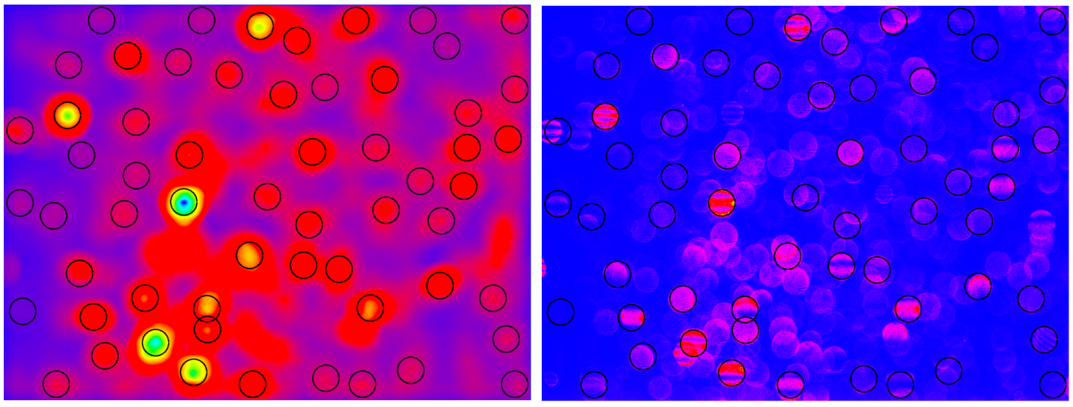

Figure 14: Convolved with a kernel with the same width as the disk diameter

intensity is a facter F larger than all points on the circle $(x - x_0)^2 + (y - y_0)^2 = (d_i/2)^2$. This leaves us with many candidate centers for each particle disk. From all candidate centers that fall within the search circle, the one with the highest intensity is picked as the center for that particle. For isolated particle images, this procedure leaves us with a complete list of particle images (Figure 14). The advantage of this method is that it works well with overlapping particles, as it will identify the brightest particle and pretty much ignore the one with lower intensity.

4.2 Determining the particle size

Once all particles have been found, the intensity can be taken among a horizontal line (Figure 15. This intensity profile $I(x)$ will resemble a noisy sine wave. To calculate the particle size, the frequency of this interference pattern is needed. Again, there are different methods to find this frequency.

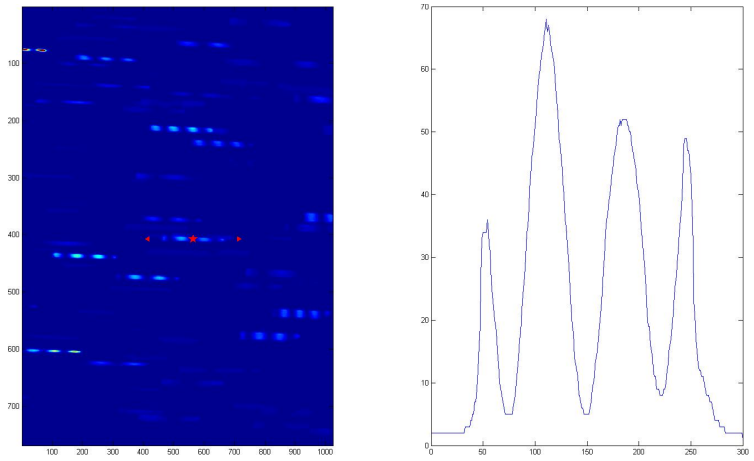

Figure 15: intensity profile along an ellipse, found using the connected pixel method

Distance between maxima

The simplest method is to determine the period of the sine wave by calculating the distance between the maxima. The signal is very noisy at first, so it needs to be filtered to reduce the amount of local peaks. Ellipses usually have a few periods in their interference pattern, so the accuracy can be slightly increased by averaging the distances between peaks. This method is still accurate at all, because the algorithm looks for points on the line which are higher then their surrounding points. Any local disturbance that remains after filtering, will result in an extra peak, which creates an error in both the amount of peaks and the distance between peaks.

Fourier analysis

Another method to determine the signals frequency is by calculating its Fourier spectrum. Again, it helps to mediate the signal, to reduce noise and reduce the amount of high frequency peaks in the spectrum. In the ideal case, the spectrum would be a single peak at the interference frequency. Of course, the situation isn't ideal, and there are also some underlying frequencies which show up in the spectrum. One of these is related to the size of the ellipse, and there is of course some noise left in the signal.

Least-squares fit

The intensity function $I(x)$ should look like

$$I(x) = a\left[(1 - \left(\frac{2x}{d_i}\right)^2\right] \frac{(1 + cos[2\pi(x/\lambda_I + \phi)}{(1 + c)}. \tag{13}$$

with a the intensity, c the fringe contrast, λ_I the fringe wavelength and ϕ the the phase. These variables can be determined using a least-squares fit.

A combination

Eventually, a combination of the latter two methods was used. By Fourier analysis the spatial wavelength λ_I and the phase ϕ can be found. But due to the optical arrangement in our experiment, and the rather small particle sizes, often no more than a few fringes are observed and further refinement of the found fringe wavelengths is necessary. This is where the least-squares process comes in. With an approximation for λ_I and ϕ known, the least squares fit can be carried out more efficiently. By placing some constraints on the intensity a and the contrast c, which are usually in the same range, the process is improved even further.

5 Results

To investigate the effect of turbulence on the droplet size probability distribution function three experiments have been performed, each under different circumstances. From the images, two measurements can be taken: The total intensity of the image is a decent good measure for the amount of particles in the laser sheet and the Particle Distribution Function can be found in the way described in chapter 4.

5.1 Constant droplet influx

The first experiment was done with a constant influx of droplets produced by the spinning disc sprayer. During the entire experiment turbulence was produced by the 8 speakers as described in section 3 using a 20 Hz noise signal.

Intensity profile

In theory, the amount of droplets should be constant when the influx of droplets by the spinning disc and the outflux by wall collisions have reached equilibrium. Figure 16 shows that the intensity is still increasing in the beginning of the measurement, which probably means the amount of particles is still increasing as well. This shows that it takes the system a little longer to reach equilibrium than anticipated.

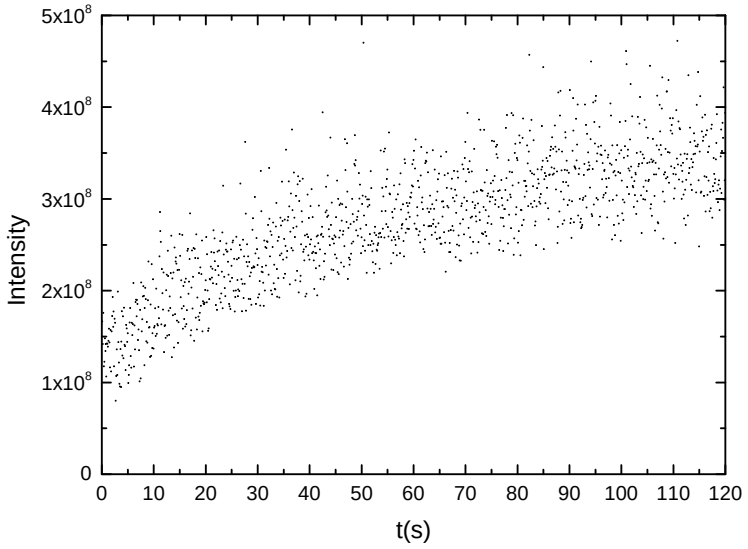

Figure 16: Intensity profile of the images in the measurement with a constant droplet influx

Particle distribution function

The particle size distribution function can be calculated for every image in the measurement. But since there are 1200 images in one measurement and there will be around 40 particles per image at maximum, it will give more insight if the PDF's of multiple images are summed up. In Figure 17 the PDF's of 200 images have been summed up, this is equal to 20 seconds of the measurement. The results show that there are more particles with sizes between 10 and 15 μm in the first 20 seconds, than in the other parts of the measurement. Perhaps the particles are around 10 micrometer at the beginning, and clutter together to bigger particles. To investigate this, the size of the droplets created by the spinning disk can be calculated from equation 10, this results in $d = 27$ μm. This is quite close to the general peak of droplet sizes, but proves nothing concerning the statement about the first 20 seconds. The smaller droplets described are most likely the satellite droplets described in chapter 2.4, which are formed as a result from training ligament breakup at the spinning disk. But the reason there are more of these satellite droplets in the first 20 seconds is still unknown, to find out more about what happens to droplets of different sizes we take a look at the second experiment.

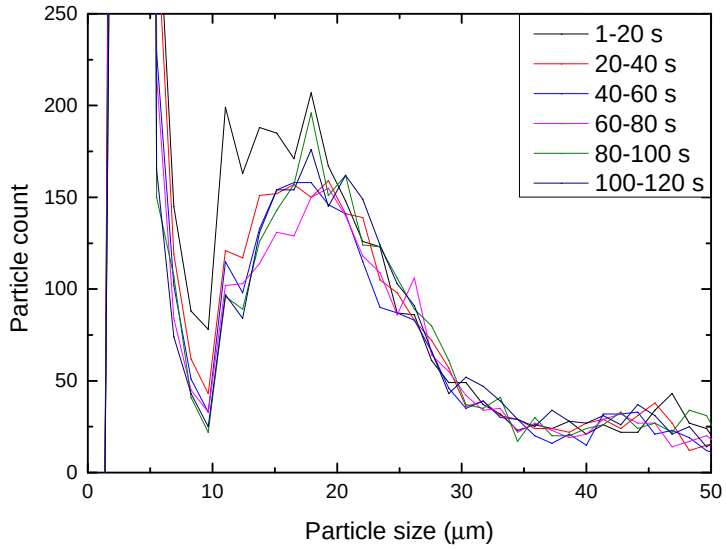

Figure 17: Particle size distribution function

5.2 With and without droplet influx

For the second experiment, the spinning disc to add water to the system was turned on at the beginning of the measurement, and turned off after approximately 60 seconds to investigate the decreasing amount of droplets due to collisions with the wall. Just like the previous measurement, turbulence was present during this entire experiment.

Intensity profile

As expected, the intensity profile shows that for the first 60 seconds, the amount of particles increases exponentially. In the second part, the amount of particles decreases exponentially, due to collisions with the wall.

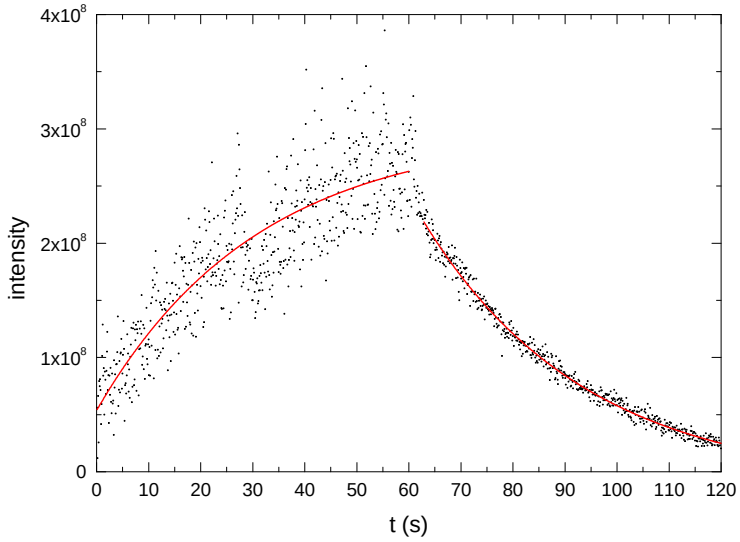

Figure 18: Intensity profile during a measurement with a constant influx of droplets during the first 60 seconds

The rate at which the intensity decreases after 60 seconds has a time constant of $\tau = 30{,}9 \pm 0{,}6$ s. To find the main reason for the decrease we calculate the time constants for both collision rates of section 2.1. This results in time constants $\tau_w = 0{,}03$ s and $\tau_p = 5 \cdot 10^5$ s for wall collisions and particle collisions respectively. So according to the theory, wall collisions should occur much more often than actually happens here. But this theory assumes every particle has a constant velocity of u_{rms}, but in reality, turbulence makes this much more complicated. The large number for τ_p shows that for particles as small as the ones we are working with happen so few that they can be neglected.
Theoretically, the first part of the measurement should increase according to the same time constant τ because the amount of droplets is limited by the same effects that cause the decrease in the second part. This curve is also

fitted in the image, and it seems that this statement is correct. Unfortunately because of the larger fluctuations in the first part this isn't very meaningful; a regular fit through the first part results in a value for $\tau = 41{,}1$ s.

Particle distribution function

The PDF for this measurement is shown in Figure 19. As can be seen, there are a lot more particles in the first half of the measurement than in the last half. What stands out from this result is the fact that the amount of particles larger than around 5 μm in the PDF decreased so rapidly between the third and fourth part, even though the intensity shows that there are more particles in the fourth part than in the first part. Note that the large peak on the left does not represent actual particle sizes, but stands for every particle that is too small for the program to find it's size, i.e. particles with less than one fringe on the image. This means the peak does stand for all the very small particles, but we do not know their exact size.

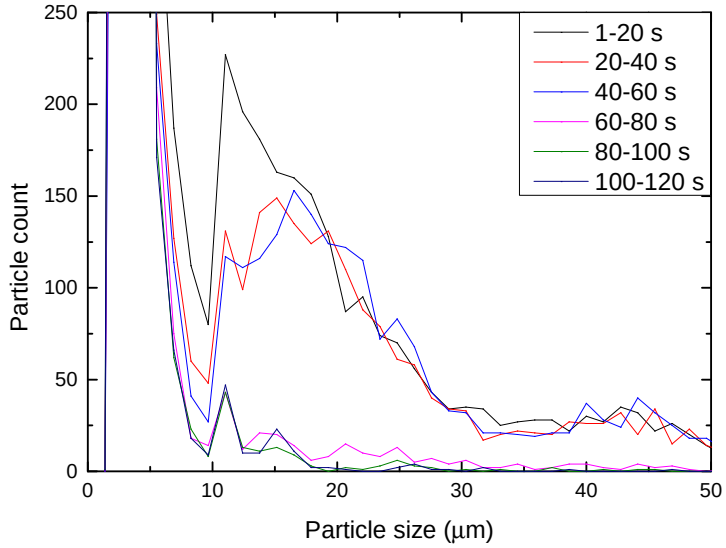

Figure 19: Particle distribution function for the measurement in which the influx of droplets was turned off after around 60 seconds (measurement nr 600)

To examine the sudden decrease in the larger particles further, the analysis was repeated for images 400 to 800, in smaller sample sizes of 50 images each. The results of this analysis is shown in Figure 20. There is still a big gap between the PDF's before and after turning off the spinning disk. Note that the images 601-650 are somewhere in between, but the influx of droplets didn't end exactly after 60 seconds, it remained on for a few images after that. So it seems like the amount of particles decreases very suddenly within a matter of seconds

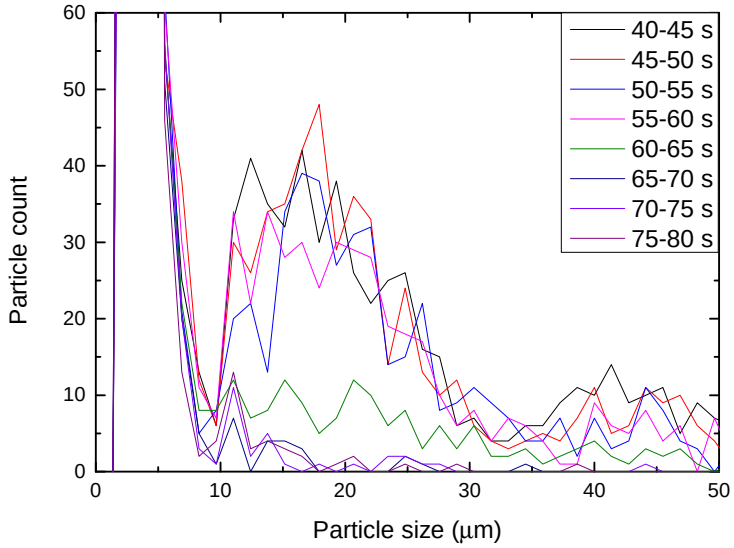

Figure 20: PDF for the same measurement, but with smaller datasets close to the point in time where the spinning disk is turned off

after the spinning disk is turned off, but the graph does not display the large peak of the smaller particles. To

show this, the amount of particles larger and smaller than 5 μm are separated and shown in Figure 21:

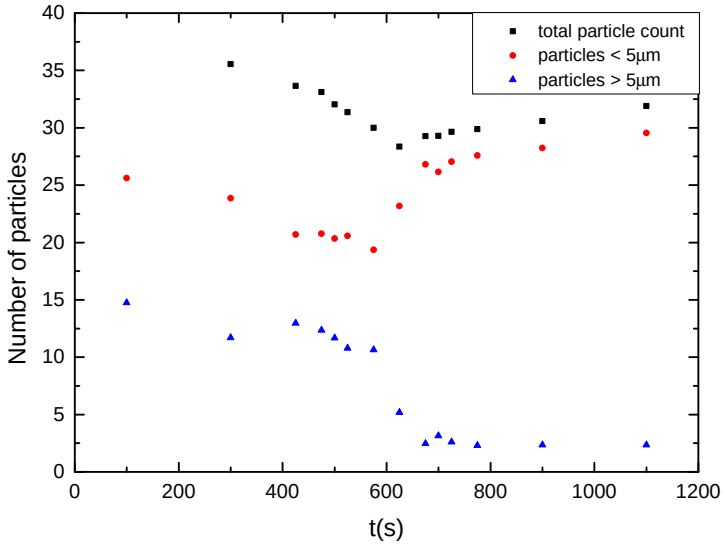

Figure 21: The average amount of droplets per image larger and smaller than 5 μm

So again, it is shown that the amount of large particles suddenly drops after the spinning disk is turned off, but the amount of small particles seems to increase. So how could most of the large droplets disappear, and more small droplets appear?

Relaxation time

One explanation could be the fact that larger particles do not follow the turbulent flow perfectly, but are smashed against the wall more often because of their higher inertia. Meanwhile, the smaller particles with less inertia follow the flow much closer. The time it takes a particle to completely follow the flow is called the relaxation time τ_r, and the distance a particle can travel in this time is the relaxation distance d_r. The relaxation time can be derived from Newtons 2^{nd} law:

$$m\frac{dv(t)}{dt} = F = 6\pi\nu v(t)d \tag{14}$$

with m the mass of the particle, $v(t)$ the velocity of a particle, $\frac{dv(t)}{dt}$ the acceleration, ν the kinematic viscosity and d it's diameter. This differential equation results in

$$v(t) = e^{-\frac{t}{\tau_r}} \tag{15}$$

with

$$\tau_r = \frac{m}{6\pi\nu d} \tag{16}$$

for the speed of the particle. Filling in the mass of a circular particle of water with density ρ results in:

$$\tau_r = \frac{\rho\frac{4}{3}\frac{1}{8}\pi d^3}{6\pi\nu d} = \frac{\rho d^2}{18\nu}. \tag{17}$$

The distance a particle can travel in this time equals

$$l_r = v(t)\tau_r = \frac{v(t)\rho d^2}{18\nu}. \tag{18}$$

The velocity of a particle isn't known in this case, but to get an idea for the order of magnitude, the rms velocity (u_{rms} = 1,73 m/s). For a small particle of around $5\mu m$ inside our measurement conditions, this means it can travel a distance of around $l_r = 100\mu m$, and the larger particles of up to 40 μm the relaxation distance reaches a maximum of around 6 mm. If a particle reaches the wall within a distance l_r, there's a good chance it's going to collide with the wall. This virtually brings the wall up to 6 mm closer to the center. This is such a small scale in a box with sides of 40 cm, that it could hardly cause the sudden decrease of large particles.

Turbophoresis

Inside the box a turbulent flow exists, with the turbulence intensity being highest in the center of the box, and decreasing towards the edges. Due to the turbulence, particles acquire a relatively high drift velocity in the direction of decreasing turbulence intensity, allowing them to drift into regions where the turbulence level is insufficiently high to supply them with the necessary momentum for the return journey [12]. This effect, which causes particles to flow from regions of high turbulence to low turbulence, is called 'Turbophoresis'. It is the inertia of the particles that causes them to be hurled outside the flow of the surrounding gas, so it's no surprise that the turbophoretic effect greatly depends on the particle size. Young and Meeling [12] summarized the contents of many experiments on the deposition of particles in turbulent pipe flow, shown in Figure (22):

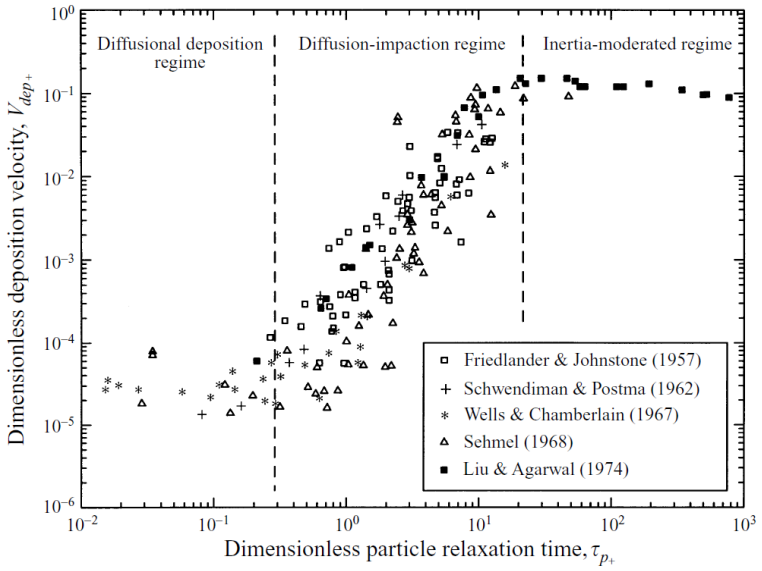

Figure 22: Particle deposition from fully developed turbulent pipe flow: a summary of experimental data

The dimensionless particle relaxation time τ_{p_+} is defined by

$$\tau_{p_+} = \tau_p u_*^2 / \nu_g \tag{19}$$

where τ_p is the particles relaxation time and ν_g is the kinematic viscosity of the gas. u_*^2 is the friction velocity, which is not known in this case, but the Kolmogorov velocity v_k is a good estimation for the friction velocity. With $\nu_g = 15{,}11 \cdot 10^{-6}\ m^2/\text{s}$ for atmospheric pressured air, and the Kolmogorov velocity $v_k = 3{,}134 \cdot 10^{-2}$ m/s, this results in $\tau_{p_+} = 0{,}09$ and $\tau_{p_+} = 1{,}46$ for particles with diameter $d = 5\ \mu$m and $d = 20\ \mu$m respectively. In figure (22) we find an estimation for the dimensionless deposition velocity V_{dep_+} of both particles, with $V_{dep_+} \approx 2 \cdot 10^{-5}$ for the small particle, and $V_{dep_+} \approx 4 \cdot 10^{-4}$ for the large particle. The dimensionless deposition velocity V_{dep_+} is defined by

$$V_{dep_+} = \frac{J_w}{\rho_{pm} u_*} \tag{20}$$

with J_w the mass flux of particles to the wall per unit area and ρ_{pm} the mean particle density in the box (mass of particles per unit volume). With ρ_{pm} and u_* being the same for both large and small particles, we can say that the mass flux of particles is directly proportional to the dimensionless deposition velocity. This means that particles of diameter $d = 20\ \mu$m flow towards the wall around 20 times faster than particles with $d = 5\ \mu$m. A difference in mass flux of this size can definitely be the cause for the amount of large droplets decreasing so much faster than the amount of small particles.

The question remains of why there are more smaller droplets appearing in the image after 60 seconds. This can probably be explained by a simple thing: The program cannot pick up every particle in the laser sheet; it is limited by the fact that the disks in the image will sometimes overlap. This means that the program will only pick up a part of all the particles, and with the amount of large particles decreasing, the amount of small particles will relatively increase.

5.3 increasing amount of droplets

To better map the effects of turbulence on the droplet sizes we need to compare the previous experiments to an experiment where there is no turbulence in the box. So for the last measurement the speakers that caused the turbulence remained off. This time, the droplet influx by the spinning disk was turned on after the measurement started, and remained on until the end of the measurement. This measurement didn't last as long as the others, as it was stopped when the image was saturated with fringe patterns.

Intensity profile

As expected, the intensity profile increases with time. In contrast to the first measurement, the intensity increases linearly, because there is no turbulence to make the particles collide with each other and with the walls.

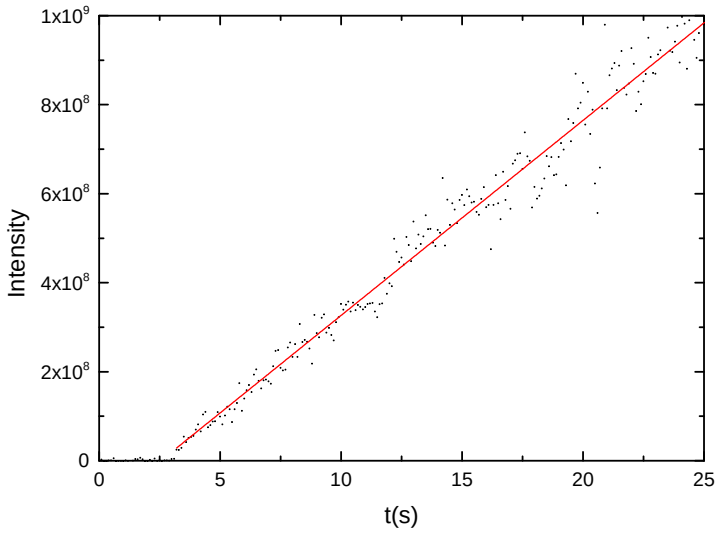

Figure 23: Intensity profile for a measurement without turbulence and continuous droplet influx

Particle distribution function

Just like the intensity measurement, the PDF shows that the amount of particles increases with time. This result is not very surprising, but comparing it with the PDF of the first measurement, there is a big difference. In the first measurement, there are hardly any droplets bigger then 30μm, while this measurement has droplets of up to 50 μm. So somehow the turbulence either stops larger droplets from forming, or destroys them when they are formed. As explained above, turbophoresis played an important role in removing particles of around 20 μm, which were all gone within a matter of seconds. For particles as large as 50 μm it follows from Figure 22 that the mass flux towards the wall is a few orders of magnitude larger, so it is quite likely that turbophoresis in the turbulent flow removes these so fast that there will hardly be any droplets of this size left in the images.

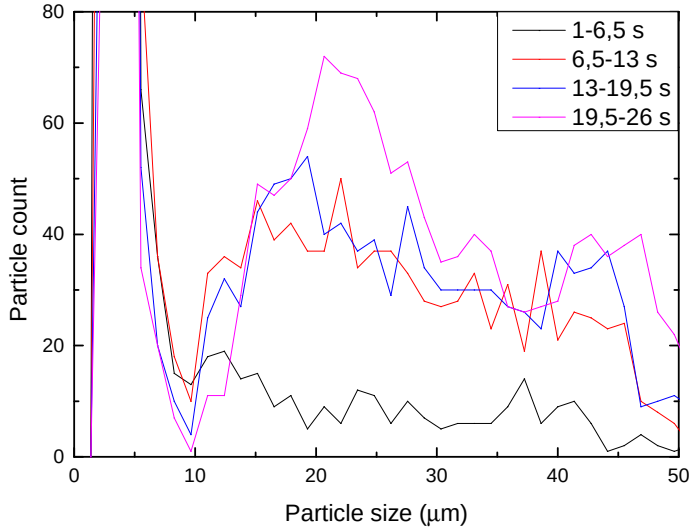

Figure 24: PDF for a measurement without turbulence and continuous droplet influx

6 Conclusion

Several methods to analyse images found by interferometric particle imaging of small droplets have been examined. In the end, finding the droplets using a wavelet transform with a circular kernel with the same diameter as the disks showed the best results. To calculate the size of the particles from these fringe patterns it was most efficient to find an approximation of the wavelength and phase of the fringes using a Fourier transform, and improving these variables with a least-squares fit. These methods resulted in accurate data for the particle sizes and a reliable method even when some of the disks overlapped in the images.

To get an idea of the total amount of particles in an image, the total intensity in each frame was used. The PDF's and intensity profiles were measured in three different situations:

The first measurement took place with a continuous influx of droplets into the turbulent flow. It seemed that the first 20 seconds, when the spinning disk had just started to add droplets to the flow, there were slightly more small particles than in the next 5 timeslots. According to the spinning disk theory, the primary diameter of droplets added to the flow should be around 27 μm, but the PDF calculations showed more small particles than expected.

In the second experiment the influx of droplets into the turbulent flow was terminated after a certain time, after which the amount of large droplets ($d > 5$ μm) rapidly decreased. With the relaxation time of all particles being so small, this could hardly be the explanation for the fact that only the large droplets quickly disappear. An effect that is more likely to be responsible for this was found in turbophoresis; the flow of droplets from regions of high turbulence to regions of lower turbulence.

When an experiment was done without turbulence inside the box and an increasing number of droplets much larger droplets of up to 50 μm were present, which weren't observed in the experiments with turbulence. With the mass flux towards the wall due to turbophoresis increasing rapidly with the relaxation time, most droplets of these sizes are already pushed towards the walls before they are even measured.

Bibliography

[1] R.A. Shaw, *Particle-Turbulence Interactions in Atmospheric Clouds.* Annu. Rev. Fluid Mech, 35:183-227, (2003)

[2] N. Damaschke, H. Nobach and C Tropea, *Optical limits of particle concentration for multi-dimensional particle sizing techniques in fluid mechanics.* Exp in Fluids 32:143-152 (2001)

[3] H.E. Albrecht, M. Borys, N Damaschke, C Tropea, *Laser doppler and phase doppler measurement techniques.* Springer-Verlag, Berlin (2003)

[4] T. Kawaguchi, Y. Akasaka and M. Maeda, *Size measurements of droplets and bubbles by advanced interferometric laser imaging technique.* Meas. Sci. Technol 13:308-316 (2002)

[5] C. Tropea, *Optical Particle Characterization in Flows.* Annu. Rev. Fluid Mech, 43:399426 (2011)

[6] E.J.P. Woittiez, H.J.J. Jonker and L.M. Portela, *On the Combined Effects of Turbulence and Gravity on Droplet Collisions in Clouds: A Numerical Study.* Journal of the atmospheric sciences, 66:1926-1943, (2009)

[7] S Inverso, *Ellipse Detection Using Randomized Hough Transform.* (2002)

[8] L. Xu, E, Oja and P. Kultanena, *A new curve detection method: Randomized hough transform (rht).* (1990)

[9] W.H. Walton, W.C. Prewett *The production of Sprays and Mists of Uniform Drop Size by Means of Spinning Disc Type Sprayers.* Proceedings of the Physical Society Section B 62(6):341:350, (1949)

[10] C.N. Davies, P.K.P. Cheah *Spinning generators of homogeneous aerosols.* Journal of Aerosol Science 15(6):719-739, (1984)

[11] H.D. Young, R.A. Freedman *University Physics.* Pearson Education, (2008)

[12] J. Young, A. Leeming *A theory of particle deposition in turbulent pipe flow.* J. Fluid Mech 340:129-159, (1997)

1 Appendix

1.1 Matlab scripts

fullloop.m

```
clc
close all
clear all
amount = 1;                  % amount of images
folder = 'D:\Studie\3e jaar\Bachelor eindproject\measurements\IPI 06-06\test spray bottle 2
ffx=0;
for i=39:39
    t = cputime;
    file= [folder 'glass00000' num2str(i,'%3.3i') '_' num2str(i,'%3.3i') '.bmp'];
    H = imread(file);
    figure, imagesc(H);

    [A,C,ff] = blobtransform(H);
    %close all
    ffx=ffx+ff;
    i
    figure, plot(ff)
    cputime-t
   end
```

blobtransform.m

```
function [A,C,ff]=blobtransform(H)
    [A,C]= findblobshorizontal(H);
    ff = Fourrier(A);
end
```

findblobshorizontal.m

```
function  [A,C, L] = findblobshorizontal(I)
% finding the blobs in the image, and returning the intensities along each
% ellipse in the columns of matrix A, and the centers in matrix C
%%
variables                                   % import variables

%Y=I(startrow:endrow,startcol:endcol);      % part of image
%% filtering image
Y=I;
B=Y;
B=medfilt2(B, [4 12]);                      % median filtering [vert hori] (original image)
if imaging
figure('Position',scrsz), imagesc(Y), title('original image')
end
                                            % min filt (segmentation image)
if imaging
figure('Position',scrsz), imagesc(Y), title('after minfilt2')
end
for R=1:numel(Y)                            % cutting off intensities below cut-value
    if Y(R) < cut
        Y(R)=0;
    %else Y(R)=1000;                        % everything above value=1000, better for segme
    end
end
Y=maxfilt2(Y, [My Mx]);
if imaging
figure('Position',scrsz), imagesc(Y), title('after cut filter')
end
```

```
%% segmentation
Allblobs=0;                                 % matrix that will hold all the found blobs (ir
%L=imrotate(bwlabel(Y,8),-1.2);             % labeling blobs and then rotating the image
L=bwlabel(Y,8);                             % without rotating
figure('position',scrsz),imagesc(L), title('BWlabel');
% finding all labels
for j=1:max(max(L));
[r,c] = find(L==j);                         % locations of pixels with label j
rc = [r c];
[sx sy]=size(rc);                           % amount of pixels found
[imx,imy]=size(B);                          % taking the size of the image
n1=zeros(imx,imy);                          % creating a matrix of the same size

% Storing the extracted image in an array
for i=1:sx
    x1=rc(i,1);
    y1=rc(i,2);
    n1(x1,y1)=1;
end                                         % Storing the extracted image in an array

if  sx > (blob)                             % if the blob is big enough

% getting the minimum and maximum of the blob in both directions
    Max = max(rc);
    Min = min(rc);
    ymax=Max(1);
    xmax=Max(2);
    ymin=Min(1);
    xmin=Min(2);
    xcenter= (xmax+xmin)/2;                 % getting the center from minima and maxima
    ycenter=(ymax+ymin)/2;

    if xcenter<(imx-Length) & xcenter>Length   % only saving it if the blob isn't near the

% storing the intensity along a line through the blob in column ncenter of A
for i=(round(xcenter)-Length):(round(xcenter)+Length-1)

    A((i+1-(round(xcenter)-Length)),ncenter)=B(round(ycenter),i);


end                                         % storing blob in A


    % storing the centers of each ellips in matrix C
    C(ncenter,1)=xcenter;
    C(ncenter,2)=ycenter;

    if imaging
    Allblobs = Allblobs+n1;                 % adding the found blobs together, not necesarr
    figure('Position',scrsz), subplot(1,2,2), plot(A(:,ncenter)), title(num2str(ncenter));
    subplot(1,2,1), imagesc(B)
    hold on
    scatter(C(ncenter,1),C(ncenter,2),200, 'red','p', 'filled')
    scatter((xcenter-Length),ycenter,50, 'red','<', 'filled')
    scatter((xcenter+Length),ycenter,50, 'red','>', 'filled')
    hold off
    end

    ncenter=ncenter+1;                      % blob counter
end
end
```

```
end % finding all labels
if exist('C')==0
    A=0;
    C=0;
    return
end

if imaging

figure('Position',scrsz), imshow(Allblobs), title('final image')
hold on
scatter(C(:,1),C(:,2),500, 'red','p', 'filled')
hold off
figure('Position',scrsz), imagesc(B), title('final image')
hold on
scatter(C(:,1),C(:,2),500, 'red','p', 'filled')
hold off
end
end



%imwrite(A, 'fourriersavedtestA.tif', 'tif');
%cputime-t
```